EINSTEIN LECTURE

Dynamical mean-field theory for correlated electrons

Dieter Vollhardt[*,**]

Electronic correlations strongly influence the properties of matter. For example, they can induce a discontinuous transition from conducting to insulating behavior. In this paper basic terms of the physics of correlated electrons are explained. In particular, I describe some of the steps that led to the formulation of a comprehensive, non-perturbative many-body approach to correlated quantum many-body systems, the dynamical mean-field theory (DMFT). The DMFT becomes exact in the limit of high lattice dimensions ($d \to \infty$) and allows one to go beyond the investigation of simple correlation models and thereby better understand, and even predict, the properties of electronically correlated materials.

1 Introduction

The average of a product of quantities usually differs from the product of the averages of the individual quantities: $\langle AB\rangle = \langle A\rangle\langle B\rangle$. The difference is, by definition, due to *correlations*. Correlations are therefore effects which go beyond the results obtained by factorization approximations such as Hartree-Fock theory.

Correlations are the essence of nature and also occur frequently in everyday life. Persons in an elevator or in a car are strongly correlated both in space and time, and it would be quite inadequate to describe the situation of a person in such a case within a factorization approximation where the influence of the other person(s) is described by a static mean-field, i.e., by a structureless cloud. For the same reason two electrons occupying the same narrow d or f orbital (which must have opposite spin due to Pauli's exclusion principle) are also strongly correlated since the effect of the Coulomb interaction between the electrons is enhanced by the spatial confinement. This is the case for many elements in the periodic table. Electrons therefore occupy narrow orbitals in numerous materials with partially filled d and f electron shells, such as the transition metals vanadium (V) and nickel (Ni) and their oxides, or rare–earth metals such as cerium (Ce).

The importance of interactions between electrons in a solid had been realized already at the outset of modern solid state physics, after de Boer and Verwey [1] had drawn attention to the surprising properties of materials with incompletely filled $3d$-bands, such as NiO. This prompted Mott and Peierls [2] to conjecture that theoretical explanations of these properties need to include the electrostatic interaction between the electrons.

Correlation effects can cause profound quantitative and qualitative changes of the physical properties of electronic systems compared to the non-interacting case. In particular, the interplay between the spin, charge, and orbital degrees of freedom of the correlated d and f electrons with the lattice degrees of freedom leads to a wealth of correlation and ordering phenomena, which include heavy fermion behavior [3], high temperature superconductivity [4], colossal magnetoresistance [5], Mott metal-insulator transitions [6], and Fermi liquid instabilities [7]. Such properties make materials with correlated electrons interesting not only for fundamental research but also for future technological applications, e.g., for the construction of tools such as sensors and switches and, more generally, for the development of electronic devices with novel functionalities [8].

---

* The author was awarded the Max Planck Medal, the highest distinction of the German Physical Society for Theoretical Physics, in 2010.

**E-mail: Dieter.Vollhardt@Physik.Uni-Augsburg.de
Theoretical Physics III, Center for Electronic Correlations and Magnetism, Institute of Physics, University of Augsburg, 86135 Augsburg, Germany

1.1 Modeling of interacting electrons

The simplest model for interacting electrons in a solid is the one-band Hubbard model, which was introduced independently by Gutzwiller, Hubbard und Kanamori [9–11]. In this model the interaction between the electrons is assumed to be purely local, i.e., very strongly screened. The Hamiltonian consists of two terms, the kinetic energy $\hat{H}_{\rm kin}$ and the interaction energy $\hat{H}_{\rm int}$ (here and in the following operators are denoted by a hat):

$$\hat{H} = \sum_{\boldsymbol{R}_i,\boldsymbol{R}_j} \sum_{\sigma} t_{ij} \hat{c}^{+}_{i\sigma} \hat{c}_{j\sigma} + U \sum_{\boldsymbol{R}_i} \hat{n}_{i\uparrow} \hat{n}_{i\downarrow} \tag{1}$$

where t_{ij} is the hopping amplitude, U is the local Hubbard interaction, $\hat{c}^{+}_{i\sigma}(\hat{c}_{i\sigma})$ are creation (annihilation) operators of electrons with spin σ at site $\boldsymbol{R}_i$, and $\hat{n}_{i\sigma} = \hat{c}^{+}_{i\sigma}\hat{c}_{i\sigma}$. The Hubbard interaction can also be written as $U\hat{D}$ where $\hat{D} = \sum_{\boldsymbol{R}_i} \hat{D}_i$, with $\hat{D}_i = \hat{n}_{i\uparrow}\hat{n}_{i\downarrow}$, is the number operator of doubly occupied sites of the system. The Fourier transform of the kinetic energy

$$\hat{H}_{\rm kin} = \sum_{\boldsymbol{k},\sigma} \epsilon_{\boldsymbol{k}} \hat{n}_{\boldsymbol{k}\sigma} \tag{2}$$

involves the dispersion $\epsilon_{\boldsymbol{k}}$ and the momentum distribution operator $\hat{n}_{\boldsymbol{k}\sigma}$. A schematic picture of the Hubbard model is shown in Fig. 1. A particular site of this lattice model can either be empty, singly occupied or doubly occupied. In particular, for strong repulsion U double occupations are energetically unfavorable and are therefore suppressed. In this situation the local correlation function $\langle \hat{n}_{i\uparrow}\hat{n}_{i\downarrow}\rangle$ must not be factorized since $\langle \hat{n}_{i\uparrow}\hat{n}_{i\downarrow}\rangle = \langle \hat{n}_{i\uparrow}\rangle\langle \hat{n}_{i\downarrow}\rangle$. Otherwise correlation phenomena are eliminated from the start. Therefore Hartree-Fock-type mean-field theories are insufficient to explain the physics of electrons in the paramagnetic phase at strong interactions.

The Hubbard model looks deceptively simple. However, the competition between the kinetic energy and the interaction leads to a complicated many-body problem, which is impossible to solve analytically, except in dimension $d = 1$ [12]. The Hubbard model provides the basis for most of the theoretical research on correlated electrons during the last decades.

2 Approximation schemes for correlated electrons

Theoretical investigations of quantum-mechanical many-body systems are faced with severe technical problems, particularly in those dimensions which are most interesting to us, i. e., $d = 2,3$. This is due to the complicated dynamics and, in the case of fermions, the nontrivial algebra introduced by the Pauli exclusion principle.

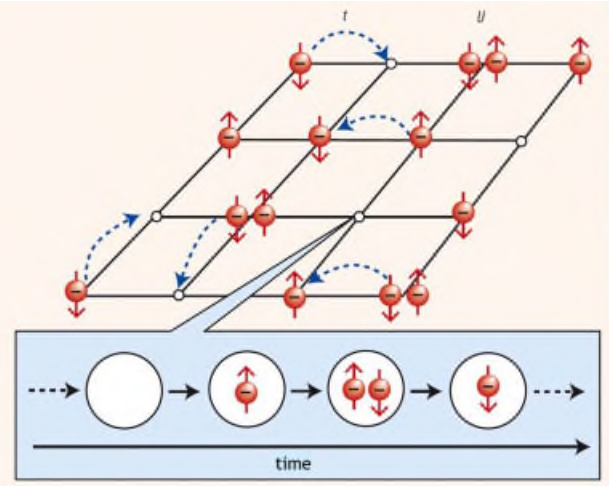

Figure 1 (online color at: www.ann-phys.org) Schematic illustration of interacting electrons in a solid in terms of the Hubbard model. The ions appear only as a rigid lattice (here represented as a square lattice). The electrons, which have a mass, a negative charge, and a spin (↑ or ↓), are quantum particles which move from one lattice site to the next with a hopping amplitude t. The quantum dynamics thus leads to fluctuations in the occupation of the lattice sites as indicated by the time sequence. When two electrons meet on a lattice site (which is only possible if they have opposite spin because of the Pauli exclusion principle) they encounter an interaction U. A lattice site can either be unoccupied, singly occupied (↑ or ↓), or doubly occupied.

In view of the fundamental limitations of exact analytical approaches one might hope that, at least, modern supercomputers can provide detailed numerical insights into the thermodynamic and spectral properties of fermionic correlation models. However, since the number of quantum mechanical states increases exponentially with the number of lattice sites L, numerically exact solutions of the Hubbard model and related models are limited to relatively small systems of the order of $L \sim 20$. This shows very clearly that there is a great need for analytically based non-perturbative approximation schemes [13], which are applicable for all input parameters.

2.1 Mean-field theories

In the theory of classical and quantum many-body systems an overall description of the properties of a model

is often obtained within a *mean-field theory*. Although the term is frequently used it does not have a very precise meaning, since there exist several quite different methods to derive mean-field theories. One construction scheme is based on a factorization of the interaction, as in the case of the Weiss mean-field theory for the Ising model, or Hartree-Fock theory for electronic models. The decoupling implies a neglect of fluctuations (or, rather, a neglect of the correlation of fluctuations; for details see [14]) and thereby reduces the original many-body problem to a solvable problem where a single spin or particle interacts with a mean field. Another, in general unrelated construction scheme makes use of the simplifications that occur when some parameter is assumed to be large (in fact, infinite), e.g., the length of the spins S, the spin degeneracy N, the number Z of nearest neighbors of a lattice site (the coordination number), or the spatial dimension d.[1] Investigations in this limit, supplemented, if possible, by an expansion in the inverse of the large parameter[2], often provide valuable insight into the fundamental properties of a system even when this parameter is not large. One of the best-known mean-field theories obtained in this way is the Weiss mean-field theory for the Ising model [15, 16]. This is a prototypical "single-site mean-field theory", which becomes exact not only in the limit $Z \to \infty$ or $d \to \infty$, but also for an infinite-range interaction. This mean-field theory contains no unphysical singularities and is applicable for all values of the input parameters, i.e., coupling parameters, magnetic field, and temperature.

2.2 Gutzwiller-Brinkman-Rice theory

Another useful approximation scheme for interacting quantum many-body systems makes use of variational wave functions [17–23]. Starting from an appropriate many-body trial wave function the energy expectation value is calculated and minimized with respect to some variational parameters. Although variational wave functions usually yield only approximate results, they have the advantage of being physically intuitive, and that they can be custom tailored to a particular problem. Furthermore, they can be used even when standard perturbation methods fail or are inapplicable.

For the analytic investigation of the model, Gutzwiller [9] proposed a very simple variational wave function, now referred to as "Gutzwiller wave function". It introduces correlations into the wave function for non-interacting particles via a purely local correlation factor in real space, which is constructed from the double occupation operator $\hat{D}$ as

$$|\Psi_G\rangle = g^{\hat{D}} \,|\,\mathrm{FS}\rangle \tag{3a}$$

$$= \prod_{\boldsymbol{R}_i} [1-(1-g)\hat{D}_i] \,|\,\mathrm{FS}\rangle, \tag{3b}$$

where $|\,\mathrm{FS}\rangle$ is the wave function of the non-interacting fermions (Fermi sea) and g is a variational parameter with $0 \le g \le 1$. The projector $g^{\hat{D}}$ globally reduces the amplitude of those spin configurations in $|\,\mathrm{FS}\rangle$ with too many doubly occupied sites. The limit $g = 1$ describes the non-interacting case, while $g \to 0$ corresponds to the strong-correlation limit. Gutzwiller introduced a further approximation [24], referred to the "Gutzwiller approximation", which allows one to calculate the corresponding ground state energy. In this approach expectation values are calculated by counting the *classical* statistical weights of different spin configurations in the non-interacting wave function. Therefore the Gutzwiller approximation corresponds to a semi-classical approximation where spatial correlations are neglected. Subsequently Brinkman and Rice [25] observed that in the case of a half-filled band the results of the Gutzwiller approximation describe a transition at a finite interaction strength U_c to a localized state, where lattice sites are singly occupied. This "Brinkman-Rice transition" therefore corresponds to a correlation induced (Mott) metal-insulator transition. The results of the Gutzwiller approximation describe a correlated, normal-state fermionic system at zero temperature, whose momentum distribution has a discontinuity q at the Fermi level which is reduced compared to the non-interacting case ($q < 1$), just as in a Landau Fermi liquid. Brinkman and Rice [25] argued that its inverse can be identified with the effective mass of Landau quasiparticles, $q^{-1} = m^*/m > 1$, which diverges at a critical value of the interaction U_c. They also extracted the Fermi liquid parameters F_0^a and F_1^s as well as [26] F_0^s as a function of the Hubbard U, and found that $F_0^s > 0$, implying a reduced compressibility, while $F_0^a < 0$, leading to an enhanced spin susceptibility. In a review article on superfluid ^{3}He, Anderson and Brinkman [27]

[1] For regular lattices both a dimension d and a coordination number Z can be defined. In this case d and Z can be used alternatively as an expansion parameter. However, there exist other lattices, such as the Bethe lattice, which cannot be associated with a physical dimension d although a coordination number Z is well-defined.

[2] In three dimensions ($d = 3$) one has $Z = 6$ for a simple cubic lattice, $Z = 8$ for a bcc lattice, and $Z = 12$ for an fcc-lattice. The parameter $1/Z$ is therefore quite small already in $d = 3$.

later noted that these theoretical results resemble the experimentally measured properties of normal liquid ^{3}He. Thus they argued that the properties of ^{3}He are determined by the incipient localization of the particles at the liquid-solid transition, i.e., that ^{3}He is "almost localized" rather than "almost ferromagnetic" as concluded within paramagnon theory [28]; similar conclusions were reached by Castaing and Nozières [29].

2.3 From the Gutzwiller approximation to infinite spatial dimensions

At this point I will briefly digress to describe how this observation by Anderson and Brinkman [27] led me to the investigation of correlated fermions. In 1982 I was a postdoc of Peter Wölfle at the Max-Planck Institute for Physics and Astrophysics, the Heisenberg Institute, in Munich. For the past three years I had enjoyed a wonderful and highly productive collaboration with Peter, especially on Anderson localization in disordered systems and spin relaxation in normal liquid ^{3}He. I was now looking for a new research topic for my habilitation thesis. During that time Bill Brinkman from Bell Laboratories visited the Technical University of Munich and met with Peter Wölfle. They also discussed about the Brinkman-Rice transition for the Hubbard lattice model and its possible connection with normal liquid ^{3}He. Peter told me about the discussion and suggested to me to study this topic more deeply. He got me interested immediately. I analyzed the quasiclassical counting of electronic spin configurations underlying the Gutzwiller approximation, worked out a connection with Fermi liquid theory, and showed that the Gutzwiller-Brinkman-Rice theory was not only in qualitative but even in good quantitative agreement with the experimentally measured properties of normal liquid ^{3}He [30]. The results of the Gutzwiller approximation clearly looked mean-field like (this is one of the reasons why the results, while obtained for the Hubbard lattice model, have a much wider range of applicability [30])[3]. As discussed in Sect. 2.1 mean-field theories can be constructed in several different ways. Therefore I asked myself whether it was possible to derive the results of the Gutzwiller approximation in a controlled way, e.g., by employing conventional methods of quantum many-body theory in some yet to be determined limit. An opportunity to investigate this problem came in 1986 when Walter Metzner, a student of physics at the Technical University of Munich, asked me for a research topic for his diploma thesis. I suggested to him to calculate the ground-state energy of the one-dimensional Hubbard model with the Gutzwiller wave function using many-body perturbation theory. Walter quickly showed that expectation values of the momentum distribution and the double occupation may be expressed as power series in the small parameter $g^2 - 1$, where g is the correlation parameter in the Gutzwiller wave function (3). The coefficients of the expansions are determined by diagrams which are identical in form to those of a conventional Φ^4 theory. However, lines in a diagram do not correspond to one-particle Green functions of the non-interacting system, $G^0_{ij,\sigma}(t)$, but to one-particle density matrices, $g^0_{ij,\sigma} = \langle \hat{c}^+_{i\sigma} \hat{c}_{j\sigma} \rangle_0 = \lim_{t\to 0^-} G^0_{ij,\sigma}(t)$. A brilliant investigation of the analytic properties of these coefficients by Walter made it possible to determine these coefficients to all orders in $d = 1$. Thus we were able to calculate the momentum distribution and the double occupation, and thereby the ground state energy of the Hubbard chain, exactly in terms of the Gutzwiller wave function [32, 33][4]. By the same method Florian Gebhard, also a diploma student of mine at that time, succeeded in analytically calculating [36, 37] four different correlation functions in $d = 1$ in terms of the Gutzwiller wave function. Our result for the spin–spin correlation function explicitly showed that in the strong coupling limit $g = 0$ the Gutzwiller wave function describes spin correlations in the nearest-neighbor, isotropic Heisenberg chain extremely well[5].

[3] Important questions concerning this approach are: Why should liquid ^{3}He be describable by a lattice model at all? And why by a model with a band filling of exactly $n = 1$? How important is the existence of an actual localization transition for the description of the properties of ^{3}He? They were addressed and clarified in a subsequent study together with Peter Wölfle and Phil Anderson where we investigated a Gutzwiller-Hubbard lattice-gas model with variable density [31].

[4] By a remarkable generalization of this technique Marcus Kollar was later able to calculate the momentum distribution and double occupation of the Hubbard model in terms of the Gutzwiller wave function in $d = 1$ even for finite magnetization [34]. At the same time he solved the recursion relation for the momentum distribution [33] in closed form. Thus we found that off half filling this variational wave function predicts ferromagnetism for strong interactions, in contrast to the exact result obtained for nearest-neighbor hopping [35].

[5] Haldane [38] and Shastry [39] independently proved that the Gutzwiller wave function with $g = 0$ is, in fact, the exact solution

Walter and I now wanted to extend the calculations to higher dimensions. But it soon became clear that analytic calculations to all orders in the power series in g^2-1 are then no longer possible. To gain insight into the behavior of the coefficients in dimensions $d > 1$ we performed the necessary sums over the internal momenta by Monte-Carlo integration. When Walter had computed the lowest-order contribution to the correlation energy for $d = 1$ up to $d = 15$ we were in for a surprise. Namely, the plot of the results as a function of d (Fig. 2) showed that for large d the value of this diagram converged to a simple result which could also be obtained by assuming the momenta carried by the lines of a diagram to be *independent*. When summed over all diagrams this approximation gave exactly the results of the Gutzwiller approximation [32, 33]. Thus we had derived the Gutzwiller approximation in a controlled, diagrammatic way. In view of the random generation of momenta in a typical Monte-Carlo integration over the momenta of a general diagram we argued that the assumption of the independence in momentum space is correct in the limit of infinite spatial dimensions ($d \to \infty$).

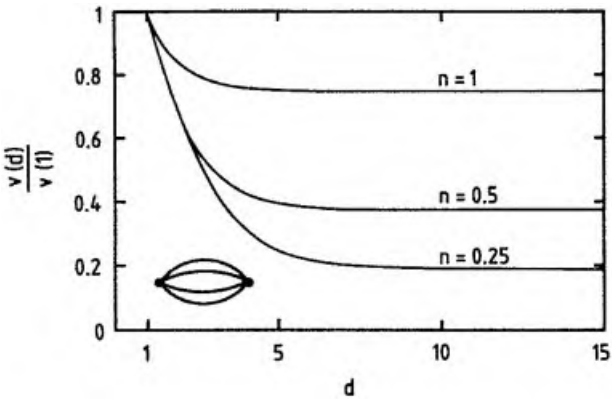

Figure 2 Value of the second-order diagram shown in the insert computed numerically for several spatial dimensions d, normalized by the value for $d = 1$, $v(1) = (2/3)(n/2)^3$, where n is the density. In the limit of high dimensions the normalized values $v(d)/v(1)$ approach the constant $3n/4$. As discussed in the text this result can also be obtained directly within a diagrammatic approximation which yields the results of the semiclassical Gutzwiller approximation; from [33].

2.3.1 Lattice fermions in high dimensions

By studying the Hubbard model with the Gutzwiller wave function Walter and I had found that diagrammatic calculations greatly simplify in the limit $d \to \infty$. Apparently this limit was not only useful for the investigation of spin models [15], but also in the case of lattice fermions. To better understand this point we analyzed the diagrams involved in the calculation of expectation values in terms of the Gutzwiller wave function in more detail. It turned out that in the limit $d \to \infty$ diagrams collapse in position space [43, 44], i.e., only local contributions remain[6]. In particular, the diagrams contributing to the proper self-energy are purely diagonal in $d = \infty$. The reason behind this collapse can be understood as follows. The one-particle density matrix may be interpreted as the amplitude for transitions between site $\boldsymbol{R}_i$ and $\boldsymbol{R}_j$. The square of its absolute value is therefore proportional to the *probability* for a particle to hop from $\boldsymbol{R}_j$ to a site $\boldsymbol{R}_i$. In the case of nearest-neighbor sites $\boldsymbol{R}_i$, $\boldsymbol{R}_j$ on a lattice with coordination number Z this implies $|\, g^0_{ij,\sigma}\,|^2 \sim \mathcal{O}(1/Z)$. For nearest-neighbor sites $\boldsymbol{R}_i$, $\boldsymbol{R}_j$ on a hypercubic lattice (where $Z = 2d$) one therefore finds for large d

$$g^0_{ij,\sigma} \sim \mathcal{O}\Big(\frac{1}{\sqrt{d}}\Big). \tag{4}$$

The general distance dependence of $g^0_{ij,\sigma}$ in the large-d limit is derived in Refs. [45, 44].

For non-interacting electrons at $T = 0$ the expectation value of the kinetic energy is given by

$$E^0_{\rm kin} = -t \sum_{\langle \boldsymbol{R}_i, \boldsymbol{R}_j \rangle} \sum_{\sigma} g^0_{ij,\sigma}. \tag{5}$$

On a hypercubic lattice the sum over the nearest neighbors leads to a factor $\mathcal{O}(d)$. In view of the $1/\sqrt{d}$ dependence of $g^0_{ij,\sigma}$ it is necessary to scale the NN-hopping amplitude t as

$$t \to \frac{t^*}{\sqrt{d}},\ t^* = \text{const.}, \tag{6}$$

since only then does the kinetic energy remain finite for $d \to \infty$. The same result is obtained in a momentum-space formulation. [7]

of the spin-1/2 antiferromagnetic Heisenberg chain with an exchange interaction which falls off as $1/r^2$; it is also identical [38] to the one-dimensional version of Anderson's "resonating valence bond" (RVB) state [40–42].

6 In other words, momentum conservation at a vertex of a skeleton diagram becomes irrelevant in the limit $d \to \infty$, implying that the momenta carried by the lines of a graph are indeed independent.

7 This is seen, for example, by calculating the density of states (DOS) of non-interacting particles. For nearest-neighbor hop-

A scaling of the microscopic parameters of the Hubbard model with d is only needed in the kinetic energy. Namely, since the interaction term is purely local, it is independent of the spatial dimension of the system and hence need not be scaled. Altogether this implies that only the Hubbard Hamiltonian with a scaled kinetic energy

$$\hat{H} = -\frac{t^*}{\sqrt{d}} \sum_{\langle \boldsymbol{R}_i, \boldsymbol{R}_j \rangle} \sum_{\sigma} \hat{c}^+_{i\sigma} \hat{c}_{j\sigma} + U \sum_{\boldsymbol{R}_i} \hat{n}_{i\uparrow} \hat{n}_{i\downarrow} \tag{7}$$

has a non-trivial $d \to \infty$ limit where both terms, the kinetic energy and the interaction, are of the same order of magnitude in d.[8]

2.3.2 Simplifications of many-body perturbation theory

The drastic simplifications of diagrammatic calculations in the limit $d \to \infty$ allowed us to calculate expectation values of the kinetic energy and the Hubbard interaction in terms of Gutzwiller-type wave functions exactly [43,44]. The result was found to be identical to the saddle point solution of the slave-boson approach to the Hubbard model by Kotliar and Ruckenstein [47]; for a brief review see [48][9].

Walter and I now wanted to understand to what extent the simplifications discovered in diagrammatic calculations with the Gutzwiller wave function in the limit $d \to \infty$ would carry over to general many-body calculations for the Hubbard model. For this purpose we evaluated the second-order diagram in Goldstone perturbation theory [52] which determines the correlation energy at weak coupling [43]. Due to the diagrammatic collapse in $d = \infty$ calculations were again found to be much simpler. Namely, the nine-dimensional integral in $d = 3$ over the three internal momenta reduces to a single integral in $d = \infty$, implying that in $d = \infty$ the calculation is simpler than in any other dimension. More importantly, the numerical value obtained in $d = \infty$ is very close to that in the physical dimension $d = 3$, and therefore provides an easily tractable, quantitatively reliable approximation (see Fig. 3).

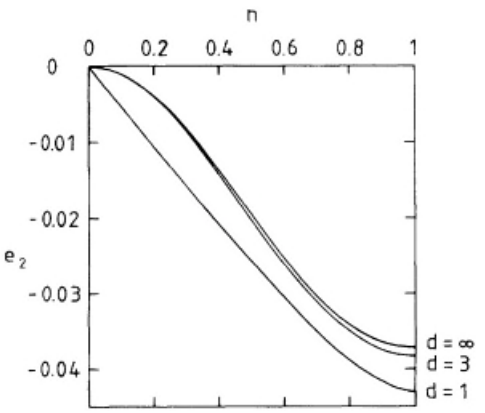

Figure 3 Correlation energy $E_c^{(2)}$ of the Hubbard model in second-order perturbation theory in U, $e_2 = E_c^{(2)}/(2U^2/|\epsilon_0|)$, vs. density n for lattice dimensions $d = 1, 3, \infty$. Here $|\epsilon_0|$ is the kinetic energy for $U = 0$ and $n = 1$; from [43].

These results clearly showed that microscopic calculations for correlated lattice fermions in $d = \infty$ dimensions were useful and very promising. Walter's and my enthusiasm about these results was shared by the colleagues whom we had told about our results early on, and

ping on a d-dimensional hypercubic lattice $\epsilon_{\boldsymbol{k}}$ has the form $\epsilon_{\boldsymbol{k}} = -2t \sum_{i=1}^{d} \cos k_i$ (here and in the following we set Planck's constant $\hbar$, Boltzmann's constant k_B, and the lattice spacing equal to unity). The DOS corresponding to $\epsilon_{\boldsymbol{k}}$ is given by $N_d(\omega) = \sum_{\boldsymbol{k}} \delta(\hbar\omega - \epsilon_{\boldsymbol{k}})$. This is just the probability density for finding the value $\omega = \epsilon_{\boldsymbol{k}}$ for a random choice of $\boldsymbol{k} = (k_1, \ldots, k_d)$. If the momenta k_i are chosen randomly, $\epsilon_{\boldsymbol{k}}$ is the sum of d many independent (random) numbers $-2t \cos k_i$. The central limit theorem then implies that in the limit $d \to \infty$ the DOS is given by a Gaussian, i.e., $N_d(\omega) \overset{d\to\infty}{\longrightarrow} \frac{1}{2t\sqrt{\pi d}} \exp\left[-\left(\frac{\omega}{2t\sqrt{d}} \right)^2 \right]$. Only if t is scaled with d as in (6) one obtains a non-trivial DOS $N_\infty(\omega)$ in $d = \infty$ [46, 43] and thus a finite kinetic energy $E^0_{\rm kin} = 2L \int_{-\infty}^{E_F} d\omega N(\omega)\omega = -2Lt^{*2} N_\infty(E_F)$, where L is the number of lattice sites.

[8] By "non-trivial limit" I mean that the competition between the kinetic energy $\hat{H}_{\rm kin}$ and the interaction $\hat{H}_{\rm int}$, expressed by $[\hat{H}_{\rm kin}, \hat{H}_{\rm int}]$, should remain finite in the limit $d \to \infty$. In the case of the Hubbard model it would be possible to employ a scaling of the hopping amplitude as $t \to t^*/d$, $t^* = \text{const.}$, but then the kinetic energy would be reduced to zero for $d \to \infty$, making the resulting model uninteresting (but not unphysical) for most purposes. For a more detailed discussion see Sect. 3 of [14].

[9] Calculations with the Gutzwiller wave function in the limit of large dimensions were cast into an optimal form by Florian Gebhard [49]. His approach has the advantage that all results in $d = \infty$ are obtained without the calculation of a single diagram. It was later generalized by him and collaborators to multi-band Hubbard model, eventually leading to a "Gutzwiller density functional theory" which can be used to describe the effect of correlations in real materials [50, 51].

who had immediately started to employ this new concept themselves. Hence only a few weeks after our paper [43] had appeared in print, Müller-Hartmann [53] proved that in infinite dimensions only on-site interactions remain dynamical, that the proper self-energy becomes momentum independent[10], $\Sigma(\boldsymbol{k},\omega) \stackrel{d\to\infty}{=} \Sigma(\omega)$, and that typical Fermi liquid features are preserved [54]. Furthermore, Schweitzer and Czycholl [55] demonstrated that practical calculations become much simpler in high dimensions also for the periodic Anderson model[11]. Shortly thereafter Brandt and Mielsch [56] obtained the exact solution of the Falicov-Kimball model for large dimensions and finite temperatures by mapping the lattice problem onto a solvable atomic problem in a generalized time-dependent external field[12]. They also noted that such a mapping is, in principle, also possible for the Hubbard model.

3 Dynamical mean-field theory for correlated lattice fermions

The limit of high spatial dimensions d or coordination number Z provides the basis for the construction of a comprehensive mean-field theory for lattice fermions described by Hubbard-type models, consisting of a kinetic energy and a purely local interaction, which is diagrammatically controlled and whose free energy has no unphysical singularities. The construction is based on the scaled Hamiltonian (7) and the simplifications in the many-body perturbation theory discussed above. Since the self-energy is momentum independent but retains the full many-body dynamics (in contrast to Hartree-Fock theory where it is merely a static potential) the resulting theory is mean-field-like *and* dynamical, and can thus describe genuine correlation effects.

The self-consistency equations of this *dynamical mean-field theory* (DMFT) for correlated lattice fermions can be derived in different ways. Nevertheless, all derivations make use of the fact that in the limit of high spatial dimensions Hubbard-type models reduce to a dynamical single-site problem, where the d-dimensional lattice model is effectively described by the dynamics of the correlated fermions on a single site which is embedded in a bath provided by the other fermions. This is illustrated in Fig. 4. The first derivation of the single-site action and the self-consistency equations of the DMFT was presented by Václav Janiš [60]. He had generalized the coherent potential approximation (CPA) for non-interacting, disordered systems[13] to lattice fermion models with local interactions and local self-energy, such as the Falicov-Kimball and Hubbard model in the limit $d = \infty$, by constructing the corresponding free energy functional (for details see [60, 61, 23, 14]). Before Václav and I could start with the numerical solution of the self-consistency equations [61] I received a preprint by Georges and Kotliar [63] in July 1991 where they formulated the DMFT by mapping the lattice problem onto a self-consistent single-impurity Anderson model. This mapping was also employed by Jarrell [64]. The DMFT equations derived within the CPA approach and the single-impurity approach, respectively, are identical. Nevertheless it is the Anderson-impurity formulation which was immediately adopted by the community since it makes contact with the well-established many-body theory of quantum impurities and Kondo problems [65], and for whose solution efficient numerical codes such as the quantum Monte-Carlo (QMC) method [66] had been developed already in the 1980's. For this reason the single-impurity based derivation of the DMFT immediately became the standard approach. The self-consistent DMFT equations are given by[14]

[10] The one-particle Green function ("propagator") $G^0_{ij,\sigma}(\omega)$ of the non-interacting system obeys the same $1/\sqrt{d}$ dependence as the one-particle density matrix $g^0_{ij,\sigma}$ (see (4)). This follows directly from $g^0_{ij,\sigma} = \lim_{t\to 0^-} G^0_{ij,\sigma}(t)$ and the fact that the scaling properties do not depend on the time evolution and the quantum mechanical representation. The Fourier transform of $G^0_{ij,\sigma}(\omega)$ also preserves this property. For this reason the same results as those obtained in the calculation with the Gutzwiller wave function hold: All connected one-particle irreducible diagrams collapse in position space, i.e., they are purely diagonal, in $d = \infty$.

[11] A more detailed presentation of the simplifications which occur in the investigation of Hubbard-type lattice models or the $t-J$ model [58, 59] in high dimensions can be found in [23].

[12] Alternatively, it can be shown that in the limit $Z \to \infty$ the dynamics of the Falicov-Kimball model reduces to that of a *non*-interacting, tight-binding model on a Bethe lattice with coordination number $Z = 3$ which can thus be solved exactly [57].

[13] For non-interacting electrons in the presence of local disorder the CPA becomes exact in the limit $d, Z \to \infty$ [62].

[14] A detailed discussion of the single-impurity based formulation of the DMFT and of the derivation of the self-consistency equations is presented in the review by Georges, Kotliar, Krauth, and Rozenberg [67]; for an introductory presentation see the article by Gabi Kotliar and myself [68].

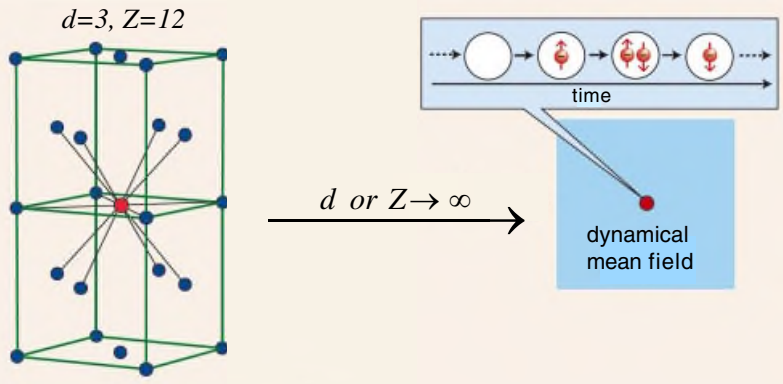

Figure 4 (online color at: www.ann-phys.org) In the limit $Z \to \infty$ the Hubbard model effectively reduces to a dynamical single-site problem, which may be viewed as a lattice site embedded in a dynamical mean field. Electrons may hop from the mean field onto this site and back, and interact on the site as in the original Hubbard model (see Fig. 1). The local propagator $G(\omega)$ (i.e., the return amplitude) and the dynamical self-energy $\Sigma(\omega)$ of the surrounding mean field play the main role in this limit. The quantum dynamics of the interacting electrons is still described exactly.

(i) The *local propagator* $G_\sigma(i\omega_n)$ which is expressed by a functional integral as

$$G_\sigma(i\omega_n) = -\frac{1}{\mathcal{Z}} \int \prod_\sigma Dc_\sigma^* Dc_\sigma [c_\sigma(i\omega_n) c_\sigma^*(i\omega_n)] \exp[-S_{\rm loc}] \tag{8}$$

with the partition function

$$\mathcal{Z} = \int \prod_\sigma Dc_\sigma^* Dc_\sigma \exp[-S_{\rm loc}] \tag{9}$$

and the local action

$$S_{\rm loc} = -\int_0^\beta d\tau_1 \int_0^\beta d\tau_2 \sum_\sigma c_\sigma^*(\tau_1) \mathcal{G}_\sigma^{-1}(\tau_1 - \tau_2) c_\sigma(\tau_2)$$

$$+ U \int_0^\beta d\tau c_\uparrow^*(\tau) c_\uparrow(\tau) c_\downarrow^*(\tau) c_\downarrow(\tau), \tag{10}$$

and where $\mathcal{G}_\sigma$ is the effective local propagator (also called "bath Green function", or "Weiss mean field")[15] which is defined by a Dyson-type equation

$$\mathcal{G}_\sigma(i\omega_n) = [[G_\sigma(i\omega_n)]^{-1} + \Sigma_\sigma(i\omega_n)]^{-1}, \tag{11}$$

(ii) and the *lattice Green function*

$$G_{\boldsymbol{k}\sigma}(i\omega_n) = \frac{1}{i\omega_n - \epsilon_{\boldsymbol{k}} + \mu - \Sigma_\sigma(i\omega_n)} \tag{12}$$

which, after performing a lattice Hilbert transform, leads to the local Green function

$$G_\sigma(i\omega_n) = \sum_{\boldsymbol{k}} G_{\boldsymbol{k}\sigma}(i\omega_n) = \int_{-\infty}^{\infty} d\epsilon \frac{N(\omega)}{i\omega_n - \epsilon + \mu - \Sigma_\sigma(i\omega_n)} \tag{13}$$

$$= G_\sigma^0(i\omega_n - \Sigma_\sigma(i\omega_n)). \tag{14}$$

In Eq. (13) the ionic lattice on which the electrons move is seen to enter only through the DOS of the non-interacting electrons. Equation (14) illustrates the mean-field character of the DMFT-equations particularly clearly: The local Green function of the interacting system is given by the *non-interacting* Green function with a renormalized energy $i\omega_n - \Sigma_\sigma(i\omega_n)$, which corresponds to the energy $i\omega_n$ measured relative to the energy of the surrounding dynamical fermionic bath, i.e., the energy of the mean field $\Sigma_\sigma(i\omega_n)$.

These are self-consistent equations of the DMFT[16] which can be solved iteratively: Starting with an initial value for the self-energy $\Sigma_\sigma(i\omega_n)$ one obtains the local propagator $G_\sigma(i\omega_n)$ from (13) and thereby the bath Green function $\mathcal{G}_\sigma(i\omega_n)$ from (11). This determines the local action (10) which is needed to compute a new value for the local propagator $G_\sigma(i\omega_n)$ from (8) and, by employing the old self-energy, a new bath Green function $\mathcal{G}_\sigma$, and so on. In spite of the fact that the solution can be obtained self-consistently there remains a complicated many-body problem which is generally not exactly solvable.

It should be stressed that although the DMFT corresponds to an effectively local problem, the propagator $G_{\boldsymbol{k}}(\omega)$ is a momentum-dependent quantity. Namely, it depends on the momentum through the dispersion $\epsilon_{\boldsymbol{k}}$ of the non-interacting electrons. However, there is no *additional* momentum-dependence through the self-energy, since this quantity is strictly local within the DMFT.

[15] In principle, the local functions $\mathcal{G}_\sigma(i\omega_n)$ and $\Sigma_\sigma(i\omega_n)$ can both be viewed as a "dynamical mean field" acting on particles on a site, since they all appear in the bilinear term of the local action (10).

[16] A generalization of the DMFT equations for the Hubbard model in the presence of local disorder was derived in [69]. In contrast to the Hubbard model spin*less* fermions with nearest-neighbor repulsion and local disorder can be treated analytically in the limit $d, Z \to \infty$ for all input parameters [70, 71].

3.1 Solution of the DMFT self-consistency equations

The dynamics of the Hubbard model remains complicated even in the limit $d \to \infty$ due to the purely local nature of the interaction. Hence an exact, analytic evaluation of the self-consistent set of equations for the local propagator G_σ or the effective propagator $\mathcal{G}_\sigma(i\omega_n)$ is not possible. A valuable semi-analytic approximation is provided by the *iterated perturbation theory* (IPT) [63, 72, 67]. Exact evaluations are only feasible when there is no coupling between the frequencies. This is the case, for example, in the Falicov-Kimball model [56, 73].

Solutions of the general DMFT self-consistency equations require extensive numerical methods, in particular quantum Monte Carlo techniques [64, 74, 75, 67, 76, 77], the numerical renormalization group [78–80], exact diagonalization [81–83] and other techniques.

It quickly turned out that the DMFT is a powerful tool for the investigation of electronic systems with strong correlations. It provides a non-perturbative and thermodynamically consistent approximation scheme for finite-dimensional systems which is particularly valuable for the study of intermediate-coupling problems where perturbative techniques fail [84, 67, 85, 68, 76].

In the following I shall discuss applications of the DMFT to problems involving electronic correlations. In particular, I will address the Mott-Hubbard metal-insulator transition, and explain the connection of the DMFT with band-structure methods – the LDA+DMFT scheme – which is the first comprehensive framework for the *ab initio* investigation of correlated electron materials.

4 The Mott-Hubbard metal-insulator transition

The correlation driven transition between a paramagnetic metal and a paramagnetic insulator, referred to as "Mott-Hubbard metal-insulator transition (MIT)", is one of the most intriguing phenomena in condensed matter physics [86–88]. This transition is a consequence of the quantum mechanical competition between the kinetic energy of the electrons and their local interaction U. Namely, the kinetic energy prefers the electrons to be mobile (a wave effect) which leads to doubly occupied sites and thereby to interactions between the electrons (a particle effect). For large values of U the doubly occupied sites become energetically very costly. The system may reduce its total energy by localizing the electrons. Hence the Mott transition is a localization-delocalization transition, demonstrating the particle-wave duality of electrons [68].

Mott-Hubbard MITs are, for example, found in transition metal oxides with partially filled bands near the Fermi level. For such systems band theory typically predicts metallic behavior. A famous example is V_2O_3 doped with Cr [89]. In particular, in $(V_{0.96}Cr_{0.04})_2O_3$ the metal-insulator transition is of first order below $T = 380$ K, with discontinuities in the lattice parameters and in the conductivity [89]. However, the two phases remain isostructural.

Making use of the half-filled, single-band Hubbard model the Mott-Hubbard MIT was studied intensively in the past [10, 90, 86–88]. Important early results were obtained by Hubbard [90] within a Green function decoupling scheme, and by Brinkman and Rice [25] who employed the Gutzwiller variational method as described in Sect. 2.2. Hubbard's approach yields a continuous splitting of the band into a lower and upper Hubbard band, but cannot describe quasiparticle features. By contrast, the Gutzwiller-Brinkman-Rice approach [30] gives a good description of the quasiparticle behavior, but cannot reproduce the upper and lower Hubbard bands. In the latter approximation the MIT is signalled by the disappearance of the quasiparticle peak. To solve this problem the DMFT has been extremely valuable since it provided detailed insights into the nature of the Mott-Hubbard MIT for all values of the interaction U and temperature T [67, 91, 68].

4.1 DMFT and the three-peak structure of the spectral function

The spectral function $A(\omega) = -\frac{1}{\pi}\mathrm{Im}G(\omega + i0^+)$ of the correlated electrons monitors the approach of the Mott-Hubbard MIT upon increase of the interaction[17]; here I follow the discussion of [68, 92]. The change of $A(\omega)$ obtained within the DMFT for the one-band Hubbard model (1.1) at $T = 0$ and half filling ($n = 1$) as a function of the Coulomb repulsion U (measured in units of the bandwidth W of non-interacting electrons) is shown in Figs. 5 and 6. While Fig. 5 is a schematic plot of the evolution of the spectrum when the interaction is increased, Fig. 6 shows actual numerical results obtained by the NRG [78, 92].

[17] In the following we only consider the paramagnetic phase, i.e, magnetic order is assumed to be suppressed ("frustrated").

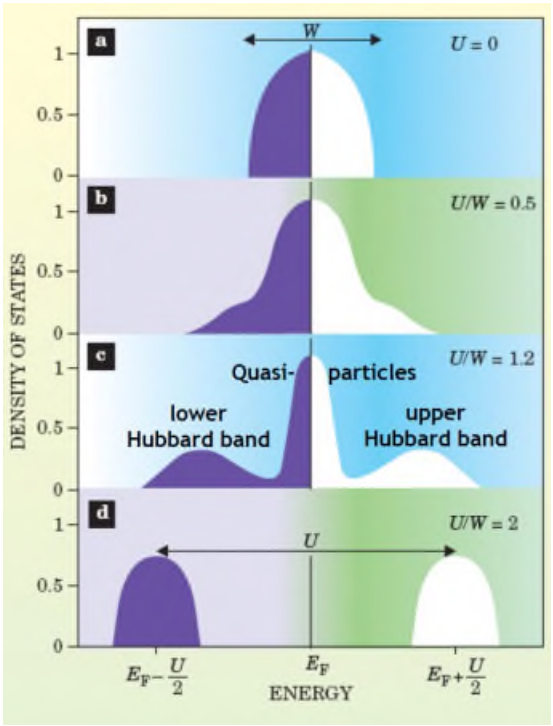

Figure 5 (online color at: www.ann-phys.org) Schematic plot of the evolution of the spectral function ("density of states") of the Hubbard model in the paramagnetic phase at half filling. a) Non-interacting case, b) for weak interactions there is only little transfer of spectral weight away from the Fermi energy, c) for strong interactions a typical three-peak structure emerges which consists of coherent quasiparticle excitations close to the Fermi energy and incoherent lower and upper Hubbard bands, d) above a critical interaction the quasiparticle peak vanishes and the system is insulating, with two well-separated Hubbard bands remaining; after [68].

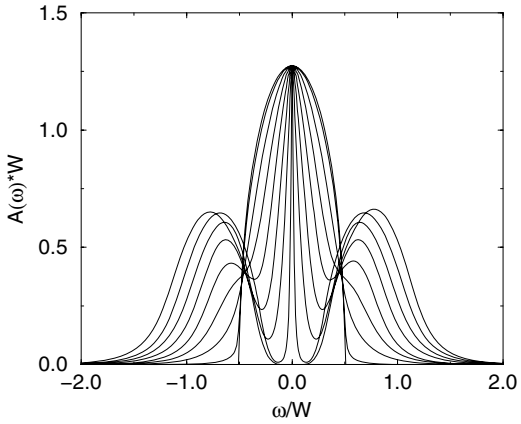

Figure 6 Numerical calculation of the evolution of the $T = 0$ spectral function of the one-band Hubbard model with a semi-elliptic ("Bethe") DOS for interaction values $U/W = 0, 0.2, 0.4, \ldots, 1.6$ (W: band width) calculated with the numerical renormalization group. At the critical interaction $U_{c2}/W \simeq 1.47$ the metallic solution disappears and the Mott gap opens; from [92].

While at small U the system can be described by coherent quasiparticles whose DOS still resembles that of the free electrons, the spectrum in the Mott insulator state consists of two separate incoherent "Hubbard bands" whose centers are separated approximately by the energy U. The latter originate from atomic-like excitations at the energies $\pm U/2$ broadened by the hopping of electrons away from the atom. At intermediate values of U the spectrum then has a characteristic three-peak structure as in the single-impurity Anderson model, which includes both the atomic features (i.e., Hubbard bands) and the narrow quasiparticle peak at low excitation energies, near $\omega = 0$. This corresponds to a strongly correlated metal. The structure of the spectrum (lower Hubbard band, quasiparticle peak, upper Hubbard band) is quite insensitive to the specific form of the DOS of the non-interacting electrons. At $T = 0$ the width of the quasiparticle peak vanishes for $U \to U_{c2}(T)$. The "Luttinger pinning" of the quasiparticle peak at $\omega = 0$ [54] is clearly observed. On decreasing U, the transition from the insulator to the metal occurs at a lower critical value U_{c1}, where the gap vanishes.

It should be noted that the three-peak structure of the spectrum discussed here originates from a lattice model (the Hubbard model) with only one type of electron. This is in contrast to the single-impurity Anderson model whose spectrum shows very similar features which are, however, due to two types of electrons, namely the localized electron at the impurity site and the itinerant conduction electrons [65]. The DMFT can explain that in the Hubbard model the same electrons provide both the local moments and the electrons which screen these moments.

At finite temperatures the thermodynamic transition line $U_c(T)$ corresponding to the Mott-Hubbard MIT is found to be of first order. It is associated with a hysteresis region in the interaction range $U_{c1} < U < U_{c2}$, where U_{c1} and U_{c2} are the values of the interaction at which physical solutions corresponding to insulating and metallic behavior, respectively, no longer exist [67, 78, 93–95, 91, 92]. The high precision MIT phase diagram by Blümer [91] is shown in Fig. 7. The hysteresis region terminates at a second-order critical point. At higher temperatures the transition changes into a smooth crossover between metallic and insulating behavior.

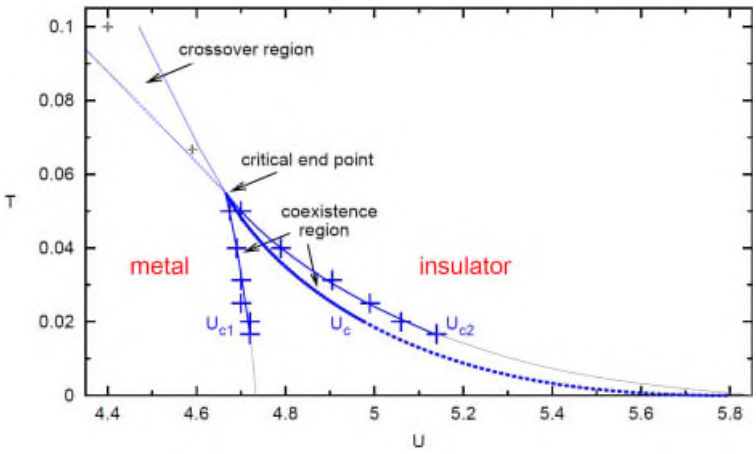

Figure 7 (online color at: www.ann-phys.org) Mott-Hubbard MIT phase diagram showing the metallic phase and the insulating phase, respectively, at temperatures below the critical end point, as well as a coexistence region; from [91].

The slope of the phase transition line is seen to be negative down to $T = 0$, which implies that for constant interaction U the metallic phase can be reached from the insulator by decreasing the temperature T, i.e., by cooling. This anomalous behavior (which corresponds to the Pomeranchuk effect [96, 97] in ^{3}He, if we associate solid ^{3}He with the insulator and liquid ^{3}He with the metal) can be easily understood from the Clausius-Clapeyron equation $dU/dT = \Delta S/\Delta D$. Here ΔS is the difference between the entropy in the metal and in the insulator, and ΔD is the difference between the number of doubly occupied sites in the two phases. Within the single-site DMFT there is no exchange coupling J between the spins of the electrons in the insulator, since the scaling (6) implies $J \propto -t^2/U \propto 1/d \to 0$ for $d \to \infty$. Hence the entropy of the macroscopically degenerate insulating state is $S_{\rm ins} = k_B \ln 2$ per electron down to $T = 0$. This is always larger than the entropy $S_{\rm met} \propto T$ per electron in the Landau Fermi-liquid describing the metal, i.e., $\Delta S = S_{\rm met} - S_{\rm ins} < 0$. At the same time the number of doubly occupied sites is lower in the insulator than in the metal, i.e., $\Delta D = D_{\rm met} - D_{\rm ins} > 0$. The Clausius-Clapeyron equation therefore implies that the phase-transition line T vs. U has a negative slope down to $T = 0$. However, this result is an artifact of the single-site approximation on which the DMFT is built. In reality a finite exchange coupling between the electrons will lead to a vanishing entropy of the insulator at $T = 0$. Since the entropy of the insulator vanishes faster than linearly with the temperature, the difference $\Delta S = S_{\rm met} - S_{\rm ins}$ will eventually become positive, whereby the slope also becomes positive at lower temperatures[18]. This is indeed observed in cluster DMFT calculations [98]. Since $\Delta S = 0$ at $T = 0$ the phase boundary must eventually terminate at $T = 0$ with infinite slope.

In correlated electronic systems with strong disorder, such as binary alloys A_xB_{1-x}, Mott-Hubbard physics as the one discussed above can take place even *off* half filling. Namely, if the binary alloy disorder is sufficiently strong, the non-interacting band splits into an upper and lower alloy subband, respectively. Krzysztof Byczuk and collaborators showed that for filling factors x or $1-x$ these alloy subbands are then half filled, such that above a critical value of the interaction strength the system becomes a Mott insulator, with a correlation gap at the Fermi level [99, 100]. Even if the disorder does not cause band splitting characteristic features of the Mott-Hubbard MIT, such as the hysteretic behavior, survive. In this case one observes the competition between Mott physics and Anderson localization [101, 102].

5 Theory of electronic correlations in materials

5.1 The LDA+DMFT approach

The Hubbard model is able to explain basic features of the phase diagram of correlated electrons, but it cannot account for the detailed physics of real materials. Indeed, realistic approaches must incorporate the explicit electronic and lattice structure of the systems.

For a long time the electronic properties of solids were investigated by two essentially separate communities, one using model Hamiltonians in conjunction with many-body techniques, the other employing density functional theory (DFT) [103, 104]. The DFT and its local density approximation (LDA) are *ab initio* approaches which do not require empirical parameters as

[18] Here we assume that the metal remains a Fermi liquid, and the insulator stays paramagnetic down to the lowest temperatures.

input, and which proved to be highly successful techniques for the calculation of the electronic structure of real materials [105]. However, in practice DFT/LDA is severely restricted in its ability to describe strongly correlated materials such as f-electron systems and Mott insulators. Here, the model Hamiltonian approach is more powerful since there exist systematic theoretical techniques to investigate the many-electron problem with increasing accuracy. Nevertheless, the uncertainty in the choice of the model parameters and the technical complexity of the correlation problem itself prevent the model Hamiltonian approach from being a flexible enough tool to study real materials. The two approaches are therefore largely complementary. In view of the individual power of DFT/LDA and the model Hamiltonian approach, respectively, a combination of these techniques for *ab initio* investigations of real materials is clearly desirable. One of the first successful attempts in this direction was the LDA+U method [106, 107], which combines LDA with a static, i.e., Hartree-Fock-like, mean-field approximation for a multi-band Anderson lattice model. This method is a very useful tool in the study of long-range ordered, insulating states of transition metals and rare-earth compounds. However, the *paramagnetic* metallic phase of correlated electron systems clearly requires a treatment that includes dynamical effects, i.e., the frequency dependence of the self-energy. Here the recently developed LDA+DMFT approach has led to significant progress in our understanding of correlated electron materials [108–117, 68]. LDA+DMFT is a computational scheme which merges electronic band structure calculations in the local density approximation (LDA) with many-body physics due to the local Hubbard interaction and Hund's rule coupling terms and then solves the corresponding correlation problem by DMFT. In 1999 Vladimir Anisimov from the Institute for Metal Physics in Ekaterinburg (Russia) and I started our collaboration on the development of the LDA+DMFT approach. Karsten Held, then a doctoral student of mine in Augsburg, took a leading role in this collaborative research and was the first author of our review of the LDA+DMFT method [113] for the Psi-k network, the international forum for cooperations in the field of electronic structure calculations.

As in the case of the simple Hubbard model the many-body model constructed within the LDA+DMFT scheme consists of two parts: a kinetic energy which describes the specific band structure of the uncorrelated electrons, and the local interactions between the electrons in the same orbital as well as in different orbitals[19]; for details see [112–117]). This complicated many-particle problem with its numerous energy bands and local interactions is then solved within DMFT, usually by the application of quantum Monte-Carlo (QMC) techniques. By construction, LDA+DMFT includes the correct quasiparticle physics and the corresponding energetics. It also reproduces the LDA results in the limit of weak Coulomb interaction U. More importantly, LDA+DMFT correctly describes the correlation induced dynamics near a Mott-Hubbard MIT and beyond. Thus, LDA+DMFT and related approaches [118, 119] are able to account for the physics at all values of the Coulomb interaction and doping.

5.2 Spectral function of correlated electrons in real materials

Transition metal oxides are an ideal laboratory for the study of electronic correlations in solids. Among these materials, cubic perovskites have the simplest crystal structure and therefore provide a good starting point for the investigation of more complex systems. Typically, the $3d$ states in those materials form comparatively narrow bands with width $W \sim 2$–3 eV, which leads to strong Coulomb correlations between the electrons. Particularly simple are transition metal oxides with a $3d^1$ configuration since, among others, they do not show a complicated multiplet structure.

Photoemission spectra provide a direct experimental tool to study the electronic structure and spectral properties of electronically correlated materials. In particular, spectroscopic studies of strongly correlated $3d^1$ transition metal oxides [6, 120–123] find a pronounced lower Hubbard band in the photoemission spectra which cannot be explained by conventional band structure theory.

5.2.1 (Sr,Ca)VO_3: a simple test material

A particularly simple correlated material which allows one to discuss the application of the LDA+DMFT approach in an exemplary way is the transition metal oxide $SrVO_3$ [121, 124]. In this material the energy band at the Fermi energy is occupied by only one $3d$ electron per

[19] It is then necessary to take into account a double counting of the interaction, since the LDA already includes some of the static contributions of the electronic interaction.

atom. One starts by calculating the electronic band structure within LDA. $SrVO_3$ has a purely cubic crystal structure with one vanadium iron per unit cell. The cubic symmetry of the crystal field splits the fivefold degenerate $3d$ orbital into a threefold degenerate t_{2g} orbital and an energetically higher lying twofold degenerate e_g orbital. In the simplest approximation only the local interaction between the electrons in the t_{2g} orbitals is included. By employing a variant of the LDA it is possible to compute the strength of the local Coulomb repulsion ($U \simeq 5.5$ eV) and the exchange-interaction ("Hund's coupling") $J \simeq 1.0$ eV. The correlated electron model defined in this way is then solved numerically within the DMFT.

Figure 8 shows the results for $SrVO_3$ together with the corresponding experimental data [125]. The local density of states of the occupied states can be measured by photoemission spectroscopy (PES). The corresponding density of states for the unoccupied states can be obtained by X-ray absorption spectroscopy (XAS). The spectra show clear signs of correlations, namely the existence of a lower and an upper Hubbard band at energies -1.5 eV and $+2.5$ eV relative to the Fermi energy E_F, as well as a pronounced maximum at the Fermi energy due to quasiparticle excitations. It should be noted that the maxima in the vicinity of the Fermi energy in the left and right part of the figure, respectively, both originate from the quasiparticle maximum and represent occupied (left) and unoccupied (right) quasiparticle states. Also shown are the results for the related compound $CaVO_3$ which is orthorhombically distorted due to the smaller Ca ion. It had long been thought that $CaVO_3$ is considerably stronger correlated than $SrVO_3$. However, the experimental data which are seen to be quite similar in both systems disprove this view [125]. The reasons for the similarity of the two spectra can be explained in detail within the LDA+DMFT approach [121].

The structure of the spectral function with its three maxima clearly shows that both $SrVO_3$ and $CaVO_3$ are strongly correlated metals. Although the DMFT had predicted such a behavior for the Hubbard model (see Sect. 5.1.) it was not clear whether this approximation would be able to provide an accurate description of real materials in three dimensions. Now we know that the three-peak structure not only occurs in single-impurity Anderson models but also in three-dimensional correlated bulk matter. Obviously the DMFT is able to give a correct explanation of the physical processes which lead to this characteristic structure.

Investigation methods based on the DMFT have proved to be a conceptual breakthrough in the realistic modeling of electronic, magnetic and structural properties of transition metals and their oxides as well as materials with f electrons [112–117, 68]. But it will take considerable further developments until it is possible to describe even complex correlated systems and predict their properties. In particular, the interface between the two main components of the LDA+DMFT approach – the band structure theory and many-body theory – need to be improved. A further important goal is the realistic calculation of the free energy of correlated solids and of microscopic forces. In parallel, the numerical tools for the solution of the complicated DMFT equations have to be continuously improved to be able to investigate materials with many energy bands and strong local interactions at very low temperatures.

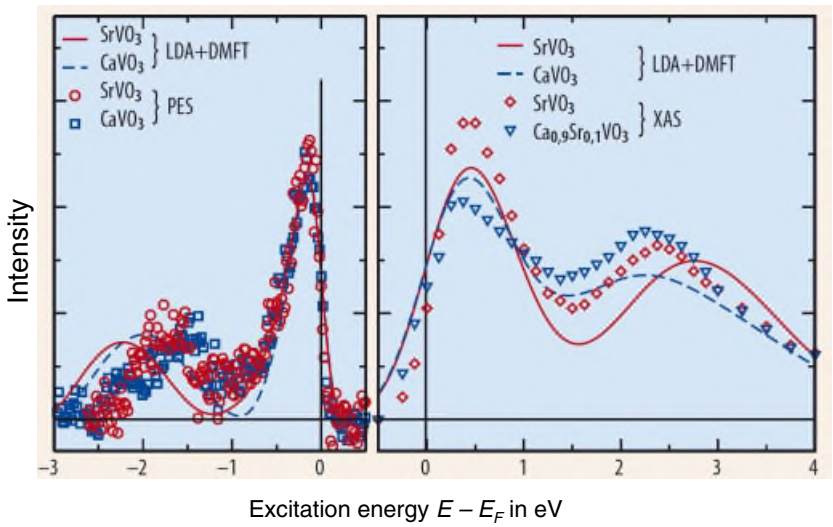

Figure 8 (online color at: www.ann-phys.org) Comparison of the calculated, parameter-free LDA+DMFT(QMC) spectra of $SrVO_3$ (solid line) and $CaVO_3$ (dashed line) with experiment. Left: Bulk-sensitive high-resolution PES ($SrVO_3$: circles; $CaVO_3$: rectangles). Right: XAS for $SrVO_3$ (diamonds) and $Ca_{0.9}Sr_{0.1}VO_3$ (triangles) [126]. Horizontal line: experimental subtraction of the background intensity; after [125].

6 Kinks in the dispersion of strongly correlated electron systems

The LDA+DMFT approach also allows one to compute $\boldsymbol{k}$-resolved spectral functions. The necessary input is a LDA-calculated Hamiltonian and the LDA+DMFT self-energy at real frequencies. The $\boldsymbol{k}$-resolved spectral function $A(\boldsymbol{k},\omega)$ calculated for $SrVO_3$ within LDA+DMFT shows two incoherent Hubbard bands and a dispersive quasiparticle band [127], which is determined by the maxima of $A(\boldsymbol{k},\omega)$. Overall the quasiparticle band is quite well described by the LDA dispersion provided the latter is renormalized by a constant factor $m^\star/m = 1.9$. This effective mass renormalization also agrees with ARPES experiments [128]. However, close to the Fermi energy the LDA+DMFT band structure is found to deviate significantly from a renormalized LDA band structure. In fact, the frequency dependence of the self-energy indicates that the actual Fermi liquid regime is restricted to a rather narrow range of energies extending from -0.2 eV to 0.15 eV. In this low-energy regime the quasiparticle mass is larger than 1.9 and corresponds to a value $m^\star_{\mathrm{low}E}/m \approx 3$. The crossover from $m^\star_{\mathrm{low}E}$ to $m^\star$ is connected with a rapid crossover in the slope of the effective dispersion relation $E_{\boldsymbol{k}}$, which is clearly visible as a "kink". What is the physical origin of this unexpected feature?

The effective dispersion relation $E_{\boldsymbol{k}}$ defines the energy and crystal momentum of one-particle excitations in a solid. For most $\boldsymbol{k}$ values $E_{\boldsymbol{k}}$ is a rather slowly varying function. Kinks are therefore quite extraordinary and carry valuable information about interactions in a many-body system. It is well-known that kinks may arise from the coupling between excitations (e.g., quasiparticles and phonons)[20], or from the hybridization of different types of fermionic excitations (e.g., d and f electrons). However, the computation of the $\boldsymbol{k}$-resolved spectral function $A(\boldsymbol{k},\omega)$ of $SrVO_3$ by DMFT discussed here [127] does not include phonons at all, and involves only t_{2g} electrons. Therefore the above mentioned coupling mechanisms do not apply.

[20] In systems with strong electron-phonon coupling the electronic dispersion routinely shows kinks at 40–60 meV below the Fermi level. When kinks were detected in the electronic dispersion of high-temperature superconductors at 40–70 meV below the Fermi level, they were therefore taken as evidence for phonon [129, 130] or spin-fluctuation based [131, 132] pairing mechanisms. But kinks are also found in the electronic dispersion of various other metals, at binding energies ranging from 30 to 800 meV [133–135], raising fundamental questions about their origins.

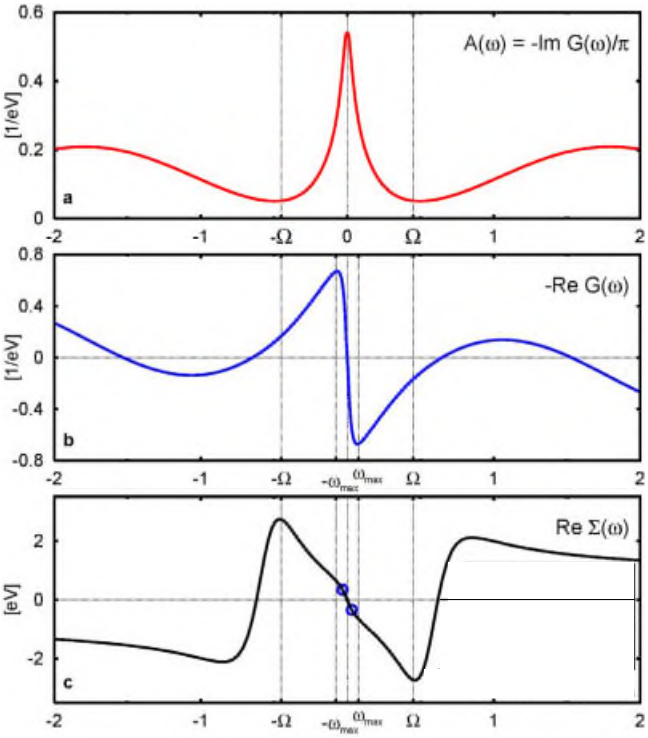

Figure 9 (online color at: www.ann-phys.org) Local propagator and self-energy for a strongly correlated system at half filling in the paramagnetic phase. (a) Correlation-induced three-peak spectral function $A(\omega) = -\mathrm{Im}\,G(\omega)/\pi$ with dips at $\pm\Omega = 0.45$ eV. (b) Corresponding real part of the propagator, $-\mathrm{Re}\,G(\omega)$, with minimum and maximum at $\pm\omega_{\max}$ inside the central spectral peak. (c) Real part of the self-energy with kinks at $\pm\omega_*$ (circles), located at the points of maximum curvature of $\mathrm{Re}\,G(\omega)$, ($\omega_* = 0.4\omega_{\max} = 0.03$ eV); after [136].

An explanation of the origin of the kink observed in the momentum-resolved spectral functions of $SrVO_3$ [127] was provided by Krzysztof Byczuk, Marcus Kollar, Karsten Held, Yi-Feng Yang, Igor Nekrasov, and myself [136]. We identified a purely electronic mechanism which leads to kinks in the electron dispersion of strongly correlated electron systems in quite a general way. Our theory applies to strongly correlated metals whose spectral function shows well separated Hubbard subbands and central peak as found, for example, in $SrVO_3$ or $CaVO_3$ (see Sect. 5.2.1). As will be explained below the origin of these kinks can be traced to the physics which is already described by the one-band Hubbard model (1.1), and the DMFT at $T = 0$ is an appropriate tool for the solution of this many-body problem [136].

The effective dispersion relation $E_{\boldsymbol{k}}$ of the one-particle excitation is determined by the singularities of the

propagator $G(\boldsymbol{k},\omega) = (\omega + \mu - \epsilon_{\mathbf{k}} - \Sigma(\boldsymbol{k},\omega))^{-1}$, which give rise to peaks in the spectral function $A(\boldsymbol{k},\omega) = -\mathrm{Im}G(\boldsymbol{k},\omega)/\pi$. Here $\epsilon_{\boldsymbol{k}}$ is the bare dispersion relation, and $\Sigma(\boldsymbol{k},\omega)$ is the self-energy which, in general, is $\boldsymbol{k}$ dependent. If the damping given by the imaginary part of $\Sigma(\boldsymbol{k},\omega)$ is not too large, the effective dispersion $E_{\boldsymbol{k}}$ is then determined by the expression

$$E_{\boldsymbol{k}} + \mu - \epsilon_{\boldsymbol{k}} - \mathrm{Re}\,\Sigma(\boldsymbol{k},E_{\boldsymbol{k}}) = 0. \tag{15}$$

Any kink in $E_{\boldsymbol{k}}$ which does not originate from $\epsilon_{\boldsymbol{k}}$ must therefore be due to changes in the slope of $\mathrm{Re}\,\Sigma(\boldsymbol{k},\omega)$.

The DMFT self-consistency equations can be used to express the self-energy (where now $\Sigma(\boldsymbol{k},\omega) \equiv \Sigma(\omega)$) as a function of $G(\omega)$; for details see [136]. As shown in Fig. 9 kinks in the slope of $\mathrm{Re}\Sigma(\omega)$ appear at a new small energy scale which emerges quite generally for a three-peak spectral function $A(\omega)$. Indeed, the Kramers-Kronig relations imply that $\mathrm{Re}\,[G(\omega)]$ is small near the dips of $A(\omega)$ located at $\pm\Omega$. Therefore $\mathrm{Re}\,[G(\omega)]$ has a maximum and a minimum at $\pm\omega_{\mathrm{max}}$ *inside the central spectral peak* (Fig. 9b). This directly leads to kinks in $\mathrm{Re}\,\Sigma(\omega)$ (Fig. 9c).

The Fermi liquid regime terminates at the kink energy scale $\omega_\star \sim \omega_{\mathrm{max}}$, which cannot be calculated within Fermi liquid theory itself. Namely, it is determined by Z_{FL} and the non-interacting DOS, e.g., $\omega_\star = 0.41 Z_{\mathrm{FL}} D$, where D is an energy scale of the non-interacting system such as half the bandwidth. One of the most surprising results of the investigations of [136] is the observation that it is possible to provide a fully analytic description of excitation frequencies which lie *outside* the Landau-Fermi-liquid regime but still within the central peak of the spectral function [136]. Above $\omega_\star$ the dispersion is given by a different renormalization with a small offset, $E_{\boldsymbol{k}} = Z_{\mathrm{CP}}\epsilon_{\boldsymbol{k}} + \mathrm{const}$, where Z_{CP} is the weight of the central peak of $A(\omega)$. The difference in the slope of the dispersions in the two energy ranges leads to the kink as is seen in Fig. 10.

The energy scale ω_* involves only the bare band structure which can be obtained, for example, from band structure calculations, and the Fermi liquid renormalization $Z_{\mathrm{FL}} = 1/(1 - \partial\mathrm{Re}\,\Sigma(0)/\partial\omega) \equiv m/m^*$ known from, e.g., specific heat measurements or many-body calculations. It should be noted that since phonons are not involved in this mechanism, $\omega_\star$ shows no isotope effect. For strongly interacting systems, in particular those close to a metal-insulator transition, $\omega_\star$ can become quite small.

The theory described above explains the kinks in the slope of the dispersion as a direct consequence of the electronic interaction. The same mechanism may also lead to kinks in the low-temperature electronic specific

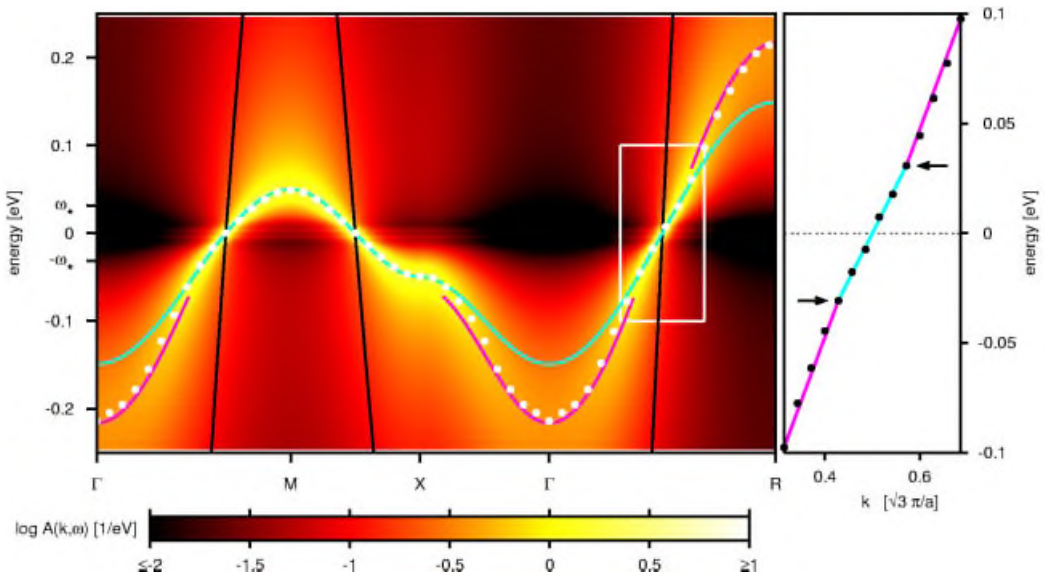

Figure 10 (online color at: www.ann-phys.org) Kinks in the dispersion relation $E_{\boldsymbol{k}}$ of the Hubbard model on a cubic lattice with interaction $U = 3.5$ eV, bandwidth $W \approx 3.46$ eV, $n = 1$, implying a Fermi-liquid renormalization factor $Z_{\mathrm{FL}} = 0.086$. The intensity plot represents the spectral function $A(\boldsymbol{k},\omega)$. Close to the Fermi energy the effective dispersion (white dots) follows the renormalized band structure $E_{\boldsymbol{k}} = Z_{\mathrm{FL}}\epsilon_{\boldsymbol{k}}$ (light line). For $|\omega| > \omega_\star$ the dispersion has the same shape but with a different renormalization, $E_{\boldsymbol{k}} = Z_{\mathrm{CP}}\epsilon_{\boldsymbol{k}} - c\ \mathrm{sgn}(E_{\boldsymbol{k}})$ (dark line). Here $\omega_\star = 0.03$ eV, $Z_{\mathrm{CP}} = 0.135$, and $c = 0.018$ eV are all calculated from Z_{FL} and $\epsilon_{\boldsymbol{k}}$ (black line). A subinterval of Γ-R (white frame) is plotted on the right, showing kinks at $\pm\omega_\star$ (arrows); after [136].

heat [137]. The kinks have also been linked to maxima in the spin susceptibility [138]. Additional kinks in the electronic dispersion may arise from the coupling of electrons to bosonic degrees of freedom, such as phonons or spin fluctuations. Recent experiments [139] have found evidence for kinks in Ni(110) at an energy which is compatible with that obtained within the framework discussed above.

7 Summary and outlook

Over the last two decades the DMFT has developed into a powerful method for the investigation of electronic systems with strong correlations. It provides a comprehensive, non-perturbative and thermodynamically consistent approximation scheme for the investigation of finite-dimensional systems (in particular for dimension $d = 3$), and is particularly useful for the study of problems where perturbative approaches are inapplicable. For this reason the DMFT has now become the standard mean-field theory for fermionic correlation problems. The generalization of this approach and its applications is currently a subject of active research. Here non-local generalizations of the DMFT play a major role. They will make it possible to study and explain even short range correlation effects which occur on the scale of several lattice constants. This also includes investigations which go beyond homogeneous systems and consider the influence of internal and external inhomogeneities such as surfaces, interfaces, thin films and multi-layered nanostructures [140–145]. An improved understanding of correlation effects in thin films and multi-layered nanostructures is particularly desirable in view of the novel functionalities of these structures and their possible applications in electronic devices.

The investigation of correlation phenomena in the field of cold atoms in optical lattices is another intriguing field of current research. Within a short time it led to the development of a versatile toolbox for the simulation and investigation of quantum mechanical many-particle systems [146–153]. While for electrons in solids the Hubbard model with its purely local interaction is a rather strong assumption, this model describes cold atoms in optical lattices very accurately since the interaction between the atoms is indeed extremely short ranged. Here the DMFT has once again proved to be extremely useful. Experiments with cold atoms in optical lattices can even access the quality of the results of the DMFT. The results obtained in this way show that the DMFT indeed leads to reliable results even for finite dimensional systems [152].

The study of models in non-equilibrium within a suitable generalization of the DMFT [154–162] has become another fascinating new research area which can be expected to explain, and even predict, the results of time-resolved spectroscopic experiments.

Above all the connection of the DMFT with conventional methods for the computation of electronic band structures has led to a conceptually new theoretical framework for the realistic modeling of correlated materials. In 10 to 15 years from now DMFT-based approaches can be expected to be as successful and standardized as the presently available density functional methods. The development of a comprehensive theoretical approach which allows physicists to quantitatively understand and predict correlation effects in materials, ranging from complex anorganic materials all the way to biological systems, is one of the great challenges for theoretical physics.

Dieter Vollhardt studied physics at the University of Hamburg during 1971–1976 and worked at the University of Southern California in Los Angeles from 1976 to 1979. He received his diploma and his doctoral degree from the University of Hamburg in 1977 and 1979, respectively. From 1979 to 1984 he was Research Associate and from 1984 to 1987 a Heisenberg-Fellow of the Deutsche Forschungsgemeinschaft at the Max-Planck-Institute for Physics and Astrophysics (Heisenberg-Institute) in Munich. During this time he also stayed at various research institutions in the US, among them, in 1983, the Institute for Theoretical Physics, Santa Barbara, and Bell Laboratories, Murray Hill. In 1984 he completed his Habilitation at the Technical University of Munich. In 1987 Dieter Vollhardt took over the Chair for Theoretical Physics C, and was appointed Director at the Institute for Theoretical Physics, at the RWTH Aachen University. In 1996 he accepted the offer for a new Chair in Theoretical Physics on Electronic Correlations and Magnetism at the Institute of Physics of the University of Augsburg. Dieter Vollhardt's main areas of research are the theory of electronic correlations and magnetism, disordered electronic systems, and normal and superfluid Helium 3.

Acknowledgements. In this article I discussed concepts and presented results obtained together with numerous collaborators during more than 20 years. I wish to express my deep gratitude to all of them, with particular thanks to Walter Metzner, and, in the chronological order of our first coauthorship, Florian Gebhard, Peter van Dongen, Václav Janiš, Ruud Vlaming, Götz Uhrig, Martin Ulmke, Karsten Held, Marcus Kollar, Nils Blümer, Walter Hofstetter, Thomas Pruschke, Vladimir Anisimov, Ralf Bulla, Igor Nekrasov, Theo Costi, Volker Eyert, Georg Keller, Krzysztof Byczuk, Jim Allen, Shigemasa Suga, Martin Ulmke, Gabi Kotliar, Ivan Leonov, Martin Eckstein, V. Dobrosavljević, and Jan Kuneš. I am also deeply grateful to Peter Wölfle for our continued collaborations over the years. Finally I thank the Deutsche Forschungsgemeinschaft for support through the Transregio TRR 80 and the Research Unit FOR 1346.

Key words. Correlated lattice fermions, dynamical mean-field theory.

References

[1] J. H. de Boer and E. J. W. Verwey, Proc. Phys. Soc. **49**(4S), 59 (1937).
[2] N. F. Mott and R. Peierls, Proc. Phys. Soc. Lond. A **49**, 72 (1937).
[3] N. Grewe and F. Steglich, in: Handbook on the Physics and Chemistry of Rare Earths, Vol. 14, edited by K. A. Gschneidner Jr. and L. Eyring (North Holland, Amsterdam, 1991) p. 343.
[4] J. R. Schrieffer, Handbook of High-Temperature Superconductivity, edited by J. R. Schrieffer (Springer, Berlin, 2007).
[5] E. Dagotto, Nanoscale Phase Separation and Collossal Magnetoresistance (Springer, Berlin, 2002).
[6] M. Imada, A. Fujimori, and Y. Tokura, Rev. Mod. Phys. **70**, 1039 (1998).
[7] H. v. Löhneysen, A. Rosch, M. Vojta, and P. Wölfle, Rev. Mod. Phys. **79**, 1015 (2007).
[8] Y. Tokura, Phys. Today, Juli 2003, p. 50.
[9] M. C. Gutzwiller, Phys. Rev. Lett. **10**, 159 (1963).
[10] J. Hubbard, Proc. Roy. Soc. London **A276**, 238 (1963).
[11] J. Kanamori, Prog. Theor. Phys. **30**, 275 (1963).
[12] E. Lieb and F. Y. Wu, Phys. Rev. Lett. **20**, 1445 (1968).
[13] P. Fulde, Electron Correlations in Molecules and Solids (Springer, Berlin, 1995).
[14] D. Vollhardt, in: Lectures on the Physics of Strongly Correlated Systems XIV, AIP Conference Proceedings, Vol. 1297, edited by by A. Avella and F. Mancini (American Institute of Physics, Melville, 2010) p. 339; arXiv:1004.5069v3.
[15] H. E. Stanley, in: Phase Transitions and Critical Phenomena, Vol. 3, edited by C. Domb and M. S. Green (Academic Press, London, 1974) p. 485.
[16] R. J. Baxter, Exactly Solved Models in Statistical Mechanics (Academic Press, London, 1982).
[17] E. Feenberg, Theory of Quantum Fluids (Academic, New York, 1969).
[18] R. P. Feynman, Statistical Physics (Benjamin, Reading, 1972).
[19] V. R. Pandharipande and R. B. Wiringa, Rev. Mod. Phys. **51**, 821 (1979).
[20] J. Bardeen, L. N. Cooper, and J. R. Schrieffer, Phys. Rev. **108**, 1175 (1957).
[21] R. B. Laughlin, Phys. Rev. Lett. **50**, 1395 (1983).
[22] For a brief review of variational wave functions for correlated electron systems see D. Vollhardt, in: Interacting Electrons in Reduced Dimensions, edited by D. Baeriswyl and D. Campbell (Plenum Press, New York, 1989) p. 107.
[23] D. Vollhardt, in: Correlated Electron Systems, edited by V. J. Emery (World Scientific, Singapore, 1993) p. 57; http://www.physik.uni-augsburg.de/theo3/Research/-research_jerusalem.vollha.en.shtml.
[24] M. C. Gutzwiller, Phys. Rev. **137**, A1726 (1965).
[25] W. F. Brinkman and T. M. Rice, Phys. Rev. B **2**, 4302 (1970).
[26] T. M. Rice and W. F. Brinkman, in: Alloys, Magnets, and Superconductors, edited by R. E. Mills, E. Ascher, and R. Jaffee (McGraw-Hill, New York, 1971) p. 593.
[27] P. W. Anderson and W. F. Brinkman, in: The Physics of Liquid and Solid Helium, Part II, edited by K. H. Bennemann and J. B. Ketterson (Wiley, New York, 1978) p. 177.
[28] K. Levin and O. T. Valls, Phys. Rep. **98**, 1 (1983).
[29] B. Castaing and P. Nozières, J. Phys. (Paris) **40**, 257 (1979).
[30] D. Vollhardt, Rev. Mod. Phys. **56**, 99 (1984).
[31] D. Vollhardt, P. Wölfle, and P. W. Anderson, Phys. Rev. B **35**, 6703 (1987).
[32] W. Metzner and D. Vollhardt, Phys. Rev. Lett. **59**, 121 (1987).
[33] W. Metzner and D. Vollhardt, Phys. Rev. B **37**, 7382 (1988).
[34] M. Kollar and D. Vollhardt, Phys. Rev. B **65**, 155121 (2002).
[35] E. H. Lieb and D. Mattis, Phys. Rev. **125**, 164 (1962).
[36] F. Gebhard and D. Vollhardt, Phys. Rev. Lett. **59**, 1472 (1987).
[37] F. Gebhard and D. Vollhardt, Phys. Rev. B **38**, 6911 (1988).
[38] F. D. M. Haldane, Phys. Rev. Lett. **60**, 635 (1988).
[39] B. S. Shastry, Phys. Rev. Lett. **60**, 639 (1988).
[40] P. W. Anderson, Mater. Res. Bull. **8**, 153 (1973).
[41] P. Fazekas and P. W. Anderson, Philos. Mag. **30**, 432 (1974).
[42] P. W. Anderson, G. Baskeran, Z. Zou, and T. Hsu, Phys. Rev. Lett. **58**, 2790 (1987).
[43] W. Metzner and D. Vollhardt, Phys. Rev. Lett. **62**, 324 (1989).

[44] W. Metzner, Z. Phys. B **77**, 253 (1989).
[45] P. G. J. van Dongen, F. Gebhard, and D. Vollhardt, Z. Phys. **76**, 199 (1989).
[46] U. Wolff, Nucl. Phys. B **225**, 391 (1983).
[47] G. Kotliar and A. E. Ruckenstein, Phys. Rev. Lett. **57**, 1362 (1986).
[48] D. Vollhardt, P. G. J. van Dongen, F. Gebhard, and W. Metzner, Mod. Phys. Lett. B **4**, 499 (1990).
[49] F. Gebhard, Phys. Rev. B **41**, 9452 (1990).
[50] J. Bünemann, F. Gebhard, and W. Weber, Found. Phys. **30**, 2011 (2000).
[51] W. Weber, J. Bünemann, and F. Gebhard, in: Band-ferromagnetism, edited by K. Baberschke, M. Donath and W. Nolting, (Springer, Berlin, 2001) p. 9.
[52] W. Metzner and D. Vollhardt, Phys. Rev. B **39**, 4462 (1989).
[53] E. Müller-Hartmann, Z. Phys. B **74**, 507 (1989).
[54] E. Müller-Hartmann, Z. Phys. B **76**, 211 (1989).
[55] H. Schweitzer and G. Czycholl, Solid State Commun. **69**, 171 (1989).
[56] U. Brandt and C. Mielsch, Z. Phys. B **75**, 365 (1989).
[57] P. G. J. van Dongen and D. Vollhardt, Phys. Rev. Lett. **65**, 1663 (1990).
[58] W. Metzner, P. Schmit, and D. Vollhardt, Phys. Rev. B **45**, 2237 (1992).
[59] R. Strack and D. Vollhardt, Phys. Rev. B **46**, 13852 (1992).
[60] V. Janiš, Z. Phys. B **83**, 227 (1991).
[61] V. Janiš and D. Vollhardt, Int. J. Mod. Phys. B **6**, 731 (1992).
[62] R. Vlaming and D. Vollhardt, Phys. Rev. B **45**, 4637 (1992).
[63] A. Georges and G. Kotliar, Phys. Rev. B **45**, 6479 (1992).
[64] M. Jarrell, Phys. Rev. Lett. **69**, 168 (1992).
[65] A. C. Hewson, The Kondo Problem to Heavy Fermions (Cambridge University Press, Cambridge, 1993).
[66] J. E. Hirsch and R. M. Fye, Phys. Rev. Lett. **56**, 2521 (1986).
[67] A. Georges, G. Kotliar, W. Krauth, and M. J. Rozenberg, Rev. Mod. Phys. **68**, 13 (1996).
[68] G. Kotliar and D. Vollhardt, Phys. Today **3**, 53 (2004).
[69] V. Janiš and D. Vollhardt, Phys. Rev. B **46**, 15712 (1992).
[70] R. Vlaming, G. S. Uhrig, and D. Vollhardt, J. Phys., Condens. Matter **4**, 7773 (1992).
[71] R. Vlaming and G. S. Uhrig, J. Phys., Condens. Matter **5**, 2561 (1993).
[72] X. Y. Zhang, M. J. Rozenberg, and G. Kotliar, Phys. Rev. Lett. **70**, 1666 (1993).
[73] J. K. Freericks and V. Zlatić, Rev. Mod. Phys. **75**, 1333 (2003).
[74] M. J. Rozenberg, X. Y. Zhang, and G. Kotliar, Phys. Rev. Lett. **69**, 1236 (1992).
[75] A. Georges and W. Krauth, Phys. Rev. Lett. **69**, 1240 (1992).
[76] Th. Maier, M. Jarrell, Th. Pruschke, and M. H. Hettler, Rev. Mod. Phys. **77**, 1027 (2005).
[77] E. Gull et al., Rev. Mod. Phys. **83**, 349 (2011).
[78] R. Bulla, Phys. Rev. Lett. **83**, 136 (1999).
[79] W. Hofstetter, Phys. Rev. Lett. **85**, 1508 (2000)
[80] R. Bulla, T. A. Costi, and Th. Pruschke, Rev. Mod. Phys. **80**, 395 (2008).
[81] M. Caffarel and W. Krauth, Phys. Rev. Lett. **72**, 1545 (1994).
[82] Q. Si, M. J. Rozenberg, G. Kotliar, and A. E. Ruckenstein, Phys. Rev. Lett. **72**, 2761 (1994).
[83] M. J. Rozenberg, G. Moeller, and G. Kotliar, Mod. Phys. Lett. B **8**, 535 (1994).
[84] Th. Pruschke, M. Jarrell, and J. K. Freericks, Adv. Phys. **44**, 187 (1995).
[85] A. Georges, in: Lectures on the Physics of Highly Correlated Electron Systems VIII, edited by A. Avella and F. Mancini, AIP Conference Proceedings, Vol. 715 (American Institute of Physics, Melville, 2004) p. 3.
[86] N. F. Mott, Rev. Mod. Phys. **40**, 677 (1968).
[87] N. F. Mott, Metal–Insulator Transitions, 2nd edition (Taylor and Francis, London, 1990).
[88] F. Gebhard, The Mott Metal-Insulator Transition (Springer, Berlin, 1997).
[89] D. B. McWhan et al., Phys. Rev. B **2**, 1920 (1973).
[90] J. Hubbard, Proc. R. Soc. Lond. A **281**, 401 (1964).
[91] N. Blümer, Metal–Insulator Transition and Optical Conductivity in High Dimensions (Shaker Verlag, Aachen, 2003).
[92] D. Vollhardt et al., J. Phys. Soc. Jpn. **74**, 136 (2005).
[93] M. J. Rozenberg, R. Chitra, and G. Kotliar, Phys. Rev. Lett. **83**, 3498 (1999).
[94] J. Joo and V. Oudovenko, Phys. Rev. B **64**, 193102 (2001).
[95] R. Bulla, T. A. Costi, and D. Vollhardt, Phys. Rev. B **64**, 045103 (2001).
[96] D. Vollhardt and P. Wölfle, The Superfluid Phases of Helium 3 (Taylor and Francis, London, 1990).
[97] C. Enss and S. Hunklinger, Low-Temperature Physics (Springer, Berlin, 2010).
[98] H. Park, K. Haule, and G. Kotliar, Phys. Rev. Lett. **101**, 186403 (2008).
[99] K. Byczuk, M. Ulmke, and D. Vollhardt, Phys. Rev. Lett. **90**, 196403 (2003).
[100] K. Byczuk, W. Hofstetter, and D. Vollhardt, Phys. Rev. B **69**, 045112 (2004).
[101] K. Byczuk, W. Hofstetter, and D. Vollhardt, Phys. Rev. Lett. **94**, 056404 (2005).
[102] K. Byczuk, W. Hofstetter, and D. Vollhardt, in: Fifty Years of Anderson Localization, edited by E. Abrahams (World Scientific, Singapore, 2010) p. 473; reprinted in Int. J. Mod. Phys. B **24**, 1727 (2010).
[103] P. Hohenberg and W. Kohn, Phys. Rev. **136B**, 864 (1964).
[104] W. Kohn and L. J. Sham, Phys. Rev. **140**, A1133 (1965).

[105] R. O. Jones and O. Gunnarsson, Rev. Mod. Phys. **61**, 689 (1989).
[106] V. I. Anisimov, J. Zaanen, and O. K. Andersen, Phys. Rev. B **44**, 943 (1991).
[107] V. I. Anisimov, F. Aryasetiawan, and A. I. Lichtenstein, J. Phys., Condens. Matter **9**, 767 (1997).
[108] V. I. Anisimov et al., J. Phys., Condens. Matter. **9**, 7359 (1997).
[109] A. I. Lichtenstein and M. I. Katsnelson, Phys. Rev. B **57**, 6884 (1998).
[110] I. A. Nekrasov et al., Eur. Phys. J. B **18**, 55 (2000).
[111] K. Held et al., Int. J. Mod. Phys. B **15**, 2611 (2001).
[112] A. I. Lichtenstein, M. I. Katsnelson, and G. Kotliar, in: Electron Correlations and Materials Properties, edited by A. Gonis, N. Kioussis, and M. Ciftan (Kluwer Academic/Plenum, New York, 2002) p. 428.
[113] K. Held et al., Psi-k Newsletter **56**, 65 (2003); reprinted in Phys. Status Solidi B **243**, 2599 (2006).
[114] G. Kotliar et al., Rev. Mod. Phys. **78**, 865 (2006).
[115] K. Held, Adv. Phys. **56**, 829 (2007).
[116] M. I. Katsnelson et al., Rev. Mod. Phys. **80**, 315 (2008).
[117] J. Kuneš et al., Eur. Phys. J. Special Topics **180**, 5 (2010).
[118] S. Biermann, F. Aryasetiawan, and A. Georges, Phys. Rev. Lett. **90**, 086402 (2003).
[119] J. Minár et al., Phys. Rev. B **72**, 45125 (2005).
[120] A. Fujimori et al., Phys. Rev. Lett. **69**, 1796 (1992).
[121] A. Sekiyama et al., Phys. Rev. Lett. **93**, 156402 (2004).
[122] D. Schrupp et al., Europhys. Lett. **70**, 789 (2005).
[123] T. C. Koethe et al., Phys. Rev. Lett. **97**, 116402 (2006).
[124] E. Pavarini et al., Phys. Rev. Lett. **92**, 176403 (2004).
[125] I. A. Nekrasov et al., Phys. Rev. B **72**, 155106 (2005).
[126] I. H. Inoue et al., Physica C **235–240**, 1007 (1994).
[127] I. A. Nekrasov et al., Phys. Rev. B **73**, 155112 (2006).
[128] T. Yoshida et al., Phys. Rev. Lett. **95**, 146404 (2005).
[129] A. Lanzara et al., Nature **412**, 510 (2001).
[130] Z.-X. Shen, A. Lanzara, S. Ishihara, and N. Nagaosa, Philos. Mag. B **82**, 1349 (2002).
[131] H. He et al., Phys. Rev. Lett. **86**, 1610 (2001).
[132] J. Hwang, T. Timusk, and G. D. Gu, Nature **427**, 714 (2004).
[133] M. Hengsberger et al., Phys. Rev. Lett. **83**, 592 (1999).
[134] E. Rotenberg, J. Schaefer, and S. D. Kevan, Phys. Rev. Lett. **84**, 2925 (2000).
[135] J. Schäfer et al., Phys. Rev. Lett. **92**, 097205 (2004).
[136] K. Byczuk et al., Nature Phys. **3**, 168 (2007).
[137] A. Toschi, M. Capone, C. Castellani, and K. Held, Phys. Rev. Lett. **102**, 076402 (2009).
[138] C. Raas, P. Grete, and G. S. Uhrig, Phys. Rev. Lett. **102**, 076406 (2009).
[139] A. Hofmann et al., Phys. Rev. Lett. **102**, 187204 (2009).
[140] M. Potthoff and W. Nolting, Phys. Rev. B **59**, 2549 (1999).
[141] J. K. Freericks, Transport in Multilayered Nanostructures – The Dynamical Mean-field Approach (Imperial College Press, London, 2006).
[142] M. Takizawa et al., Phys. Rev. Lett. **97**, 057601 (2006).
[143] L. Chen and J. K. Freericks, Phys. Rev. B **75**, 1251141 (2007).
[144] K. Byczuk, in: Condensed Matter Physics in the Prime of the 21st Century: Phenomena, Materials, Ideas, Methods, edited by J. Jedrzejewski (World Scientific, Singapore, 2008) p. 1.
[145] R. W. Helmes, T. A. Costi, and A. Rosch, Phys. Rev. Lett. **100**, 056403 (2008).
[146] D. Jaksch et al., Phys. Rev. Lett. **81**, 3108 (1998).
[147] W. Hofstetter et al., Phys. Rev. Lett. **89**, 220407 (2002).
[148] M. Greiner et al., Nature **415**, 39 (2002).
[149] A. Rapp, G. Zarand, C. Honerkamp, and W. Hofstetter, Phys. Rev. Lett. **98**, 160405 (2007).
[150] M. Snoek et al., New J. Phys. **10**, 093008 (2008).
[151] R. Jördens et al., Nature **455**, 204 (2008).
[152] U. Schneider et al., Science **322**, 1520 (2008).
[153] I. Bloch, J. Dalibard, and W. Zwerger, Rev. Mod. Phys. **80**, 885 (2008).
[154] V. Turkowski and J. K. Freericks, Phys. Rev. B **71**, 085104 (2005).
[155] J. K. Freericks, V. M. Turkowski, and V. Zlatić, Phys. Rev. Lett. **97**, 266408 (2006).
[156] J. K. Freericks, Phys. Rev. B **77**, 075109 (2008).
[157] N. Tsuji, T. Oka, and H. Aoki, Phys. Rev. B **78**, 235124 (2008).
[158] M. Eckstein and M. Kollar, Phys. Rev. Lett. **100**, 120404 (2008).
[159] M. Eckstein and M. Kollar, Phys. Rev. B **78**, 205119 (2008).
[160] J. K. Freericks, H. R. Krishnamurthy, and Th. Pruschke, Phys. Rev. Lett. **102**, 136401 (2009).
[161] M. Eckstein, M. Kollar, and P. Werner, Phys. Rev. Lett. **103**, 056403 (2009).
[162] M. Eckstein and P. Werner, Phys. Rev. B **82**, 115115 (2010).